TOXICOLOGICAL SCIENCES **98(1)**, 145–158 (2007)
doi:10.1093/toxsci/kfm084
Advance Access publication April 10, 2007

Ketamine-Induced Neuronal Cell Death in the Perinatal Rhesus Monkey

William Slikker Jr,*,[1] Xiaoju Zou,* Charlotte E. Hotchkiss,† Rebecca L. Divine,‡ Natalya Sadovova,‡ Nathan C. Twaddle,§ Daniel R. Doerge,§ Andrew C. Scallet,* Tucker A. Patterson,* Joseph P. Hanig,¶ Merle G. Paule,* and Cheng Wang*

*Division of Neurotoxicology, National Center for Toxicological Research, U.S. Food & Drug Administration †Bionetics Corporation; ‡Toxicologic Pathology Associates; §Division of Biochemical Toxicology, National Center for Toxicological Research, U.S. Food & Drug Administration, Jefferson, Arkansas 72079; and ¶Division of Applied Pharmacology Research, Center for Drug Evaluation and Research, U.S. Food & Drug Administration, Silver Spring, Maryland 20993

Received February 15, 2007; accepted March 23, 2007

Ketamine is widely used as a pediatric anesthetic. Studies in developing rodents have indicated that ketamine-induced anesthesia results in brain cell death. Additional studies are needed to determine if ketamine anesthesia results in brain cell death in the nonhuman primate and if so, to begin to define the stage of development and the duration of ketamine anesthesia necessary to produce brain cell death. Rhesus monkeys ($N = 3$ for each treatment and control group) at three stages of development (122 days of gestation and 5 and 35 postnatal days [PNDs]) were administered ketamine intravenously for 24 h to maintain a surgical anesthetic plane, followed by a 6-h withdrawal period. Similar studies were performed in PND 5 animals with 3 h of ketamine anesthesia. Animals were subsequently perfused and brain tissue processed for analyses. Ketamine (24-h infusion) produced a significant increase in the number of caspase 3–, Fluoro-Jade C– and silver stain–positive cells in the cortex of gestational and PND 5 animals but not in PND 35 animals. Electron microscopy indicated typical nuclear condensation and fragmentation in some neuronal cells, and cell body swelling was observed in others indicating that ketamine-induced neuronal cell death is most likely both apoptotic and necrotic in nature. Ketamine increased N-methyl-D-aspartate (NMDA) receptor NR1 subunit messenger RNA in the frontal cortex where enhanced cell death was apparent. Earlier developmental stages (122 days of gestation and 5 PNDs) appear more sensitive to ketamine-induced neuronal cell death than later in development (35 PNDs). However, a shorter duration of ketamine anesthesia (3 h) did not result in neuronal cell death in the 5-day-old monkey.

Key Words: **NMDA receptor; ketamine; neurotoxicology; apoptosis; development; anesthetic agents; nonhuman primate.**

Ketamine produces a dose-related state of unconsciousness and analgesia commonly referred to as dissociative anesthesia (Kohrs and Durieux, 1998). Ketamine's role in pediatric anesthesia is well established (Haberny *et al.*, 2002; Mellon *et al.*, 2007). Recent studies on anesthetics have shown that clinically relevant doses of ketamine, a noncompetitive N-methyl-D-aspartate (NMDA) receptor antagonist, trigger massive and widespread apoptotic neurodegeneration in the immature rat brain (Ikonomidou *et al.*, 1999; Scallet *et al.*, 2004). Because of the complexity and temporal features associated with normal brain development, it has been hypothesized that the developing nervous system may be more susceptible than the mature brain to some neurotoxic insults. During development in the rat, the window of vulnerability to the toxic effects of ketamine is restricted to the period of rapid synaptogenesis, also known as the brain growth spurt, which occurs immediately after neurons have differentiated and migrated to their final destinations (postnatal days [PNDs] 1–14). It is postulated that, in rodents, excessive suppression of neuronal activity by ketamine during the brain growth spurt triggers neuronal apoptosis.

NMDA receptors are widely distributed throughout the central nervous system (CNS) and operate ligand-activated ion channels primarily composed of three families of NMDA receptor subunits: NR1 with eight splice variants, NR2 (A–D) (Kutsuwada *et al.*, 1992; Monyer *et al.*, 1992; Moriyoshi *et al.*, 1991), and NR3A and B (Nishi *et al.*, 2001; Wong *et al.*, 2002). The NR1 subunit is essential for receptor/channel function. The functional properties of the NMDA receptor vary throughout the CNS and the binding affinities of various ligands for recombinant NMDA receptors depend on subunit composition (Laurie and Seeburg, 1994). NMDA receptors are involved in a variety of physiological and pathological processes, including memory and learning (Collingridge *et al.*, 1983), neuronal development (D'Souza *et al.*, 1993), epileptiform seizures, synaptic plasticity (Meldrum and Garthwaite, 1990), and acute neuropathologies associated with strokes and other trauma-related events (Beal, 1992).

Disclaimer: This document has been reviewed in accordance with U.S. FDA policy and approved for publication. Approval does not signify that the contents necessarily reflect the position or opinions of the FDA nor does mention of trade names or commercial products constitute endorsement or recommendation for use. The findings and conclusions in this report are those of the authors and do not necessarily represent the views of the FDA.

[1] To whom correspondence should be addressed at National Center for Toxicological Research, HFT-1, Food & Drug Administration, Jefferson, AR 72079-0502. Fax: (870) 543-7576. E-mail: william.slikker@fda.hhs.gov.

Blockade of NMDA receptors is known to cause neuronal cell death in some instances, but the underlying mechanisms involved in such effects are unknown. The administration of noncompetitive NMDA receptor antagonists such as ketamine, phencyclidine (PCP), and MK-801 to rats during a critical period of development results in neuronal cell death in several major brain areas (Ikonomidou *et al.*, 1999; Scallet *et al.*, 2004). In 1999, Olney and coworkers demonstrated severe widespread apoptosis throughout the rapidly developing brain of the 7-day-old rat pup after ketamine administration. Our previous studies have also demonstrated that repeated administration of PCP to rodents (7–14 days of age) results in a sensitized locomotor response in rats subjected to later PCP challenge (Johnson *et al.*, 1998). This sensitization is associated with apoptotic cell death and an increase in NMDA receptor NR1 subunit messenger RNA (mRNA) and NMDA receptor immunoreactivity in rat forebrain (Hanania *et al.*, 1999; Wang *et al.*, 1999, 2005a). PCP-induced neuronal cell loss and associated deficits in acoustic startle prepulse inhibition can be attenuated by treatment with a superoxide dismutase mimetic, M40403 (Wang *et al.*, 2003), suggesting an important role of superoxide anions in NMDA antagonist-induced apoptosis and behavioral alterations.

The issue of whether ketamine-induced neuronal cell death seen in rodents is relevant for children would be informed if similar effects were seen in a developing nonhuman primate. The present study was designed to (1) determine whether ketamine anesthesia produces elevated neuronal cell death in the developing monkey; (2) determine the most sensitive stages of development during which ketamine increases neuronal cell death; (3) observe the anesthetic duration below which no significant neuronal cell death can be detected; and (4) investigate whether such ketamine-induced cell loss is associated with altered NMDA receptor function/composition or mRNA in developing monkeys.

MATERIALS AND METHODS

Drugs and Other Materials

Ketamine hydrochloride (Ketaset®, Fort Dodge Animal Health, Fort Dodge, IA) was diluted in lactated Ringer's solution. Ketamine was identified and its purity confirmed (> 99%) with high-performance liquid chromatography and mass spectrometry (LC/MS). Antisense oligodeoxynucleotide probes (for the NMDA receptor NR1 subunit) were synthesized by and obtained from Sigma Genosys Biotechnologies, Inc. (The Woodlands, TX).

Animals

All animal procedures were approved by the National Center for Toxicological Research (NCTR) Institutional Animal Care and Use Committee and conducted in full accordance with the PHS Policy on Humane Care and Use of Laboratory Animals. The breeding colony consisted of natural-habitat–reared rhesus macaques (*Macaca mulatta*, age 4–9 years; prime reproductive years) housed at NCTR, an AAALAC-accredited facility, under a 12:12-h light/dark cycle. Monkeys were provided with water *ad libitum* and fed High Protein Monkey Diet Jumbo (#5047, PMI Nutrition International, Richmond, IN) twice daily, supplemented with fresh fruit three times a week. Monkeys were housed individually when not breeding. Menstrual cycles were monitored via daily vaginal swabs (first day of bleeding = day 1) and females were transferred to a breeder male's cage over days 11–13 of the cycle. Pregnancy was confirmed by ultrasound at 30–40 days of gestation. No ketamine or other pharmaceutical agents were administered to pregnant or potentially pregnant monkeys. For the infants, mothers were allowed to deliver naturally and the day of birth was designated as PND 0. Infants remained with their mothers until the start of the study. When pregnant monkeys were used, the first day of placement with a breeder male was designated gestation day zero (GD 0).

Treatment Groups

Eighteen monkeys at three different stages of development were evaluated: nine animals after 24 h of ketamine anesthesia and nine animals after 24 h of control conditions [GD 122 (range GD 120–123), PND 5 (range PND 5–6), and PND 35 (range PND 35–37)]. An additional six PND 5 monkeys were evaluated: three animals after 3 h of ketamine anesthesia and three animals after 3 h of control conditions. In all cases, a 6-h withdrawal period was allowed before animals were deeply anesthetized (ketamine, 20 mg/kg, im), followed by transaortic perfusion of 0.9% saline and 3.7% formaldehyde in 0.1M buffer. The flow rate (10–15 ml/min) was carefully controlled by a pump controller (Masterflex®, Cole Parmer Instrument Co. Chicago, IL). The brain samples were removed immediately after perfusion.

For each age and exposure duration, monkeys were randomly assigned to treatment and control groups ($N = 3$/group).

Dosing Procedure

Immediately prior to the initiation of anesthesia, monkeys were removed from their home cage and transferred to the procedure room. Control monkeys were maintained in a holding cage with water but no food, and were not sedated for physiological measurements or blood sample collection. Samples were collected from the control animals while they were chair-restrained. For treated monkeys, ketamine was given as an initial intramuscular injection (20 mg/kg) followed by continuous intravenous infusion at a rate of 20–50 mg/kg/h to maintain a light surgical plane of anesthesia (as evidenced by lack of voluntary movement, decreased muscle tone, and minimal reaction to physical stimulation with maintenance of an intact palpebral reflex) for either 3 or 24 h. Throughout anesthesia, monkeys were kept in an incubator with a circulating water heating pad and heat lamp to maintain body temperature. Dextrose was administered (5%, 5–15 ml/kg/h) by stomach tube (infants), water bottle (control pregnant adults), or intravenously (ketamine-treated pregnant adults) to maintain blood glucose levels. Glycopyrrolate (0.01 mg/kg im) was administered prior to anesthesia and every 6 h to all monkeys (both control and treated) to reduce salivary secretions.

Maintenance of Physiological Conditions

Pulse oximetry (N-395 Pulse Oximeter, Nellcor, Pleasanton, CA), capnography (Tidal Wave Hand-held Capnograph, Respironics, Murrysville, PA), noninvasive sphygmomanometry (Critikon Dynamap Vital Signs Monitor, GE Healthcare, Waukesha, WI), and a rectal probe were used to monitor physiological conditions. Pulse rates, respiratory rates, oxygen saturation of hemoglobin, expired CO_2 concentrations, and rectal temperatures were recorded every 15 min in treated monkeys and every 1–2 h in control monkeys. Systolic, diastolic, and mean arterial blood pressure were recorded every 30 min in treated monkeys and every 2–4 h in controls. Blood (0.25 ml) was collected at 1- to 4-h intervals for the measurement of plasma ketamine, glucose (Ascension Elite XL Blood Glucose Meter, Bayer Diagnostics, Tarrytown, NY), and hematocrit.

Determination of Plasma Ketamine Concentrations

Venous blood samples were collected (approximately 0.25 ml), centrifuged, and plasma was stored frozen until analysis.

Characterization of internal standards. Solutions of ketamine hydrochloride (unlabeled 1.0 mg/ml as free base and d4-labeled 0.1 mg/ml as free base) and nor-ketamine (unlabeled 1.0 mg/ml as free base and d4-labeled 0.1 mg/ml as free base) were obtained from Cerilliant Co. (Round Rock, TX).

The concentrations of labeled species were verified by comparing LC-UV (269 nm) responses with the solutions of unlabeled analogs. No unlabeled ketamine or nor-ketamine was observed in the respective labeled analog (< 0.1%). The plot of response ratios for labeled versus unlabeled ketamine was linear over the concentration range of 0.01–2.0μM unlabeled plus 0.1μM d4-ketamine with a slope of 0.94 and a correlation coefficient of 0.999. The plot of response ratios for labeled versus unlabeled nor-ketamine was linear over the concentration range of 0.01–2.0μM unlabeled plus 0.1μM d4-nor-ketamine with a slope of 1.08 and a correlation coefficient of 0.999. Six different concentration ratios, analyzed in duplicate, were used for each plot and all back-calculated concentrations were within 10% of the nominal value.

Solid phase extraction. To 1–100 μl of plasma was added 10 μl of 1 pmol/μl labeled ketamine/nor-ketamine into a culture tube. The total volume was brought to 250 μl with ammonium acetate buffer (50mM, pH 5.0) and the solution was briefly mixed. Isolute HCX (100 mg) SPE cartridges (Biotage, Charlottesville, VA) were activated with 2 × 1 ml of methanol containing 5% (v/v) concentrated ammonia water (28% w/v) followed by 2 × 1 ml of methanol. The cartridges were then conditioned with 2 × 1 ml 50mM ammonium acetate buffer (pH 5.0) followed by aspiration of the samples. Wash steps included 250 μl of ammonium acetate buffer followed by 250 μl of 1M acetic acid. The cartridges were then allowed to dry before washing with 250 μl of methanol. The analytes were then eluted with 2 × 0.5 ml of 5% methanol containing 5% ammonia. The eluent was evaporated using reduced pressure centrifugation (Speed-Vac, Thermo, Bellefonte, PA). Samples were reconstituted in 100 μl of water and aliquots of 15–50 μl were analyzed.

Liquid chromatography. LC was performed using a Waters Acquity (Waters Co., Milford, MA) separations module in conjunction with a Luna C18(2) (2 × 150 mm, 3 μm particle size, Phenomenex, Torrance, CA) analytical column and a SecurityGuard precolumn (Phenomenex). The isocratic mobile phase consisted of 85:15 0.01% aqueous formic acid:methanol (v/v) at a flow rate of 0.2 ml/min. All separations were performed at ambient temperature with a total run time of 6 min.

Mass spectrometry. Analyses were conducted using a Quattro Micro or Quattro Premier triple quadrupole mass spectrometer (Waters, Milford, MA) equipped with an electrospray source. Positive ions were monitored in selected ion recording mode. Source and desolvation temperatures were set to 100°C and 300°C, respectively with dwell times of 0.2 s. Capillary potential was 0.5 kV. Resolution was set to give peak widths at half-height of 0.9 Th. Optimized *m/z* ratios were acquired (*m/z* 242-labeled ketamine, *m/z* 238-unlabeled ketamine and *m/z* 228-labeled nor-ketamine, *m/z* 224-unlabeled nor-ketamine) using cone voltages of 25 and 20 V, respectively, for quantification of the protonated molecules from ketamine and nor-ketamine. In addition, two pairs of confirmatory ions were acquired for ketamine (*m/z* 211.1-labeled, *m/z* 207.1 unlabeled) and nor-ketamine (*m/z* 170.1-labeled, *m/z* 166.1-unlabeled).

Method performance. The method described was optimized with respect to the solid phase extraction cartridges, solvents, and laboratory hardware available to give the highest recoveries based on fortified samples (> 80%) and MS response. Limits of detection and quantification for ketamine and nor-ketamine were approximately 6 and 17 pg on column, respectively. When using 10-μl plasma samples, this corresponds to concentrations of approximately 0.0012 and 0.0036 μg/ml, respectively (0.005 and 0.014μM).

Method validation. The method was validated for accuracy and precision over 2 days using 10 μl of control rat plasma spiked at concentrations of 0.1, 1.0, and 5.0μM ketamine and nor-ketamine. The accuracies for ketamine were 103–114% and the intraday and interday precision was between 2% and 12%. The accuracies for nor-ketamine were 102–112% and the intraday and interday precision was between 1% and 6%.

Caspase 3 Immunocytochemistry

In order to measure the density and distribution of caspase 3, Fluoro-Jade C and silver staining positive neural cells, the following procedure was followed. After carefully reviewing the 50-μm coronal sections (for whole monkey brain including hippocampus, thalamus, striatum, amygdala, and cerebellum), it was determined that the effects of ketamine infusion (24 h) on perinatal monkey brain were mainly restricted to the cortical brain regions, especially in the frontal cortex (see "Results"). The center of the peak regions (cortical regions) of neurodegeneration that in adults would correspond to Interaural 32.70 mm and Bregma 10.80 mm (coronal section coordinates), as defined by the atlas of Rhesus Monkey Brain (Paxinos *et al.*, 2000), and adjacent pre- and post-serial sections were selected for morphological and statistical measurements.

Coronal sections (50 μm) through whole brain were cut using a vibratome, rinsed in phosphate-buffered saline (PBS) and processed for immunocytochemistry as described previously (Muller *et al.*, 1996). Briefly, sections were first washed in PBS for 1 h, permeabilized in PBS/0.5% bovine serum albumin (BSA)/0.3% triton for 30 min at room temperature and then incubated with the primary antibodies at 4°C overnight. A rabbit polyclonal antibody that detects human and mouse cleaved caspase 3 (1:200; Trevigen, Gaithersburg, MD), one of the key effectors of apoptosis, was used.

Bound antibodies were revealed with horseradish peroxidase–conjugated sheep anti-rabbit secondary antibodies (diluted 1:40, Boehringer, in PBS/0.5% BSA) for 12 h. After washing in PBS, sections were immersed in 3,3-diaminobenzidine tetrahydrochloride (Sigma, St Louis, MO), placed on slides and examined with a Nikon microscope.

Fluoro-Jade C Staining

Coronal sections (50 μm) through whole brain were cut with a vibratome, rinsed in PBS, and processed for Fluoro-Jade C staining as described previously (Schmued *et al.*, 2005). Prior to staining, sections were mounted onto subgelatinized slides which were first immersed in a basic alcohol solution consisting of 1% sodium hydroxide in 80% ethanol for 5 min followed by a wash for 2 min in 70% ethanol and in distilled water, and incubated in 0.06% potassium permanganate solution for 10 min. Slides were then transferred for 10 min to a 0.0001% solution of Fluoro-Jade C (Histo-Chem, Inc., Jefferson, AR) dissolved in 0.1% acetic acid vehicle. The proper dilution was accomplished by first making a 0.01% stock solution of the dye in distilled water and then adding 1 ml of the stock solution to 99 ml of 0.1% acetic acid vehicle. The slides were rinsed through three changes of distilled water for 1 min per change. The air dried slides were cleared in xylene and then coverslipped with DPX nonfluorescent mounting media (Sigma).

Degeneration-Selective Silver Staining

Adjacent sections (50 μm) through whole brain were cut with a vibratome, rinsed in PBS, and processed for DeOlmos silver staining as described previously (Ye *et al.*, 2001). Briefly, sections were processed in a plastic staining basket with 24 wells and a vinyl mesh bottom. Sections were rinsed and preincubated in pretreating solution (9% NaOH + 1.2% NH_4NO_3) for 10 min. Sections were incubated in impregnating solution (9% NaOH + 16% NH_4NO_3 + 50% $AgNO_3$) for 10 min then rinsed in washing solution (1.2% NH_4NO_3 + 0.05% $C_6H_8O_7$). The sections were then processed in developing solution (0.05% $C_6H_8O_7$ + 1.2% NH_4NO_3) for 1 min, bleached with 0.5% acetic acid for 10 min, and mounted onto subgelatinized slides. Finally, the slides were dehydrated in a series of ethanol washes, cleared in xylene, and coverslipped with permount medium.

Quantitative Analysis

To determine the degenerative neural cell, a PC-based Image Analysis System (MCID, Imaging Research, Inc., St Catherines, Ontario, Canada) interfaced to an Olympus Vanox microscope by way of a solid state video camera was used for image analysis. Unbiased sampling for each monkey was performed by randomly selecting five viewing fields (×10)/section from six serial frontal cortical sections collected from the same cortical location from each monkey. These viewing fields (photographs) were counted by a trained expert and later confirmed by two raters whom were blind to the treatment.

The threshold was determined interactively by consensus of two trained observers and then held constant for all viewing fields (Scallet *et al.*, 2004). The numerical density counts generated by our procedure accurately represented the silver grains visible in the original images.

TUNEL (Terminal deoxy-Uridine Triphosphate Nick-End Labeling) Assay

Condensed or fragmented DNA was assayed using TUNEL staining as previously described (Johnson *et al.*, 1998; Rabacchi *et al.*, 1994). Deoxynucleotidyl transferase (TdT), a template-independent polymerase, was used to incorporate biotinylated nucleotides at sites of DNA breaks. The signal was then amplified using avidin–biotin peroxidase, enabling conventional histochemical identification by light microscopy. In brief, brain tissues ($N = 3$/group; initially perfusion fixed) were removed from the frontal cortex (from left hemisphere; these tissues were also used for electron micrograph [EM] and *in situ* hybridization studies) and additionally fixed in ice-cold (4°C) 4% paraformaldehyde. Slide-mounted sections (10 μm) were treated with proteinase K to dissociate proteins from DNA and the sections were washed in PBS. The sections were covered with H_2O_2 to inactivate endogenous peroxidase, rinsed with PBS, and immersed in TdT buffer (30mM Tris, pH 7.2, 140mM sodium cacodylate, 1mM cobalt chloride). The reaction mixture was then replaced with TdT (0.3 U/μl; Roche, Indianapolis, IN) and biotinylated deoxy-uridine triphosphate (0.2nM/10 U TdT; Roche) in TdT buffer and incubated in a humid atmosphere at 37°C for 60 min. The reaction was terminated by transferring the sections to buffer (300mM NaCl, 30mM sodium citrate) for 15 min at room temperature. The slides were rinsed with PBS, covered with 2% BSA for 10 min at room temperature, and rinsed in PBS. The slides were covered with biotin–avidin (1:50 in PBS; Vectastain ABC kit; Vector, Burlingame, CA), incubated for 30 min at 37°C and immersed in 0.05M Tris–HCl. The reaction product was visualized with 3,3′-diaminobenzidine (Sigma).

Electron Microscopy

All brain tissues for EM study ($N = 3$/group; control and ketamine-treated) were removed from the frontal cortex (left hemisphere) and additionally fixed in ice-cold (4°C) 2% paraformaldehyde and 0.1% glutaraldehyde in 0.1M phosphate buffer (pH 7.4). The frontal cortex tissues were washed (3 × 30 min) in 0.1M phosphate buffer (pH 7.4), postfixed with 1% osmium tetroxide in 0.1M cacodylate buffer, then washed with 25% and 50% ethanol plus 5% uranyl acetate, followed by dehydration in an ascending ethanol series and embedded in Epon. The semisections (1 μm) were counterstained with Toluidine Blue dye and then examined under a Nikon light microscope. The thin sections were then counterstained with uranyl acetate and lead citrate, and randomly selected fields were examined at 60 kV using a Philips CM100 electron microscope.

In Situ Hybridization

An oligonucleotide probe complementary to the mRNA encoding the NMDA receptor NR1 subunit was selected on the basis of cloned complementary DNA sequences. The sequence of the probe used for *in situ* hybridization was as follows: 5′-TTCCTCCTCCTCCTCACTGTTCACCTT-GAATCGGC-CAAAGGGACT (this corresponds to a region that is constant across all NR1 splice variants). It was 3′ end-labeled by incubation with [^{35}S]deoxy-adenosine triphosphate (New England Nuclear, Boston, MA) and TdT (Boehringer Mannheim Corp., Indianapolis, IN) to attain specific activities of approximately 5–8 × 10 cpm/μg. The specificity of the probes has been previously described (Monyer *et al.*, 1992; Moriyoshi *et al.*, 1991).

Coronal sections (10 μm) through the frontal cortex were cut with a cryostat, rinsed in PBS, and processed for *in situ* hybridization as described previously (Bartanusz *et al.*, 1993). After an overnight hybridization at 41°C, slides were washed successively in 4×, 1×, and 0.1× SSC (sodium chloride–sodium citrate solution), quickly dehydrated in ethanol (70%), and air dried. Autoradiography was performed using Kodak (Rochester, NY) NTB3 emulsion; slides were exposed for 3 weeks at 4°C. Analysis of *in situ* hybridization autoradiographs was accomplished on hematoxylin–eosin–counterstained sections.

Quantitation of In Situ *Autoradiographs*

Images were acquired with the Microcomputer Imaging Device (MCID; Imaging Research, Inc., St Catherines, Ontario, Canada) for analysis. Briefly, the images were smoothed with a 3 × 3 square filter to remove noise, and regions of interest (ROIs) were selected using a threshold technique that segments the image into labeled cells and background (Scallet *et al.*, 2004). The threshold was held constant for all ROIs within each section. The density of silver grains associated with neurons was estimated by measuring the area within a 20-μm-fixed-diameter circle placed over individual neurons that exceeded the threshold value. Background labeling was determined in a similar fashion and was subtracted from each measurement to estimate specific labeling in each ROI. A monotonic relationship was assumed to exist between measured labeling and the amount of mRNA labeled with the radioactive probe. This technique is similar to that used by several laboratories except that a fixed size rather than a variable size ROI was used.

Statistical Analyses

The effect of ketamine treatment on physiologic endpoints and histochemical endpoints at the three stage-of-development dates (GD 122, PND 5, and PND 35) and two durations of exposure (24 and 3 h) was analyzed. The data for the 24 and 3 h exposures were analyzed separately. For the 24 h exposure, a two-way analysis of variance (ANOVA), stage of development and treatment, with a repeated measure variable was used to evaluate ketamine effect. The repeated variable is a time variable following initiation of treatment for physiologic endpoints, and the repeated variable for the histochemical points is a section variable represented various measurements made in different sections. For each stage of development and treatment combination, the post *t*-test for the treatment effect was performed. The Tukey test was used to correct for multiple comparisons. The data for the 3 h exposure at PND 5 were analyzed using a one-way ANOVA with a repeated (time or section) variable. The null hypothesis was rejected at the significance level of $p < 0.05$. All analyses were conducted using Statistical Analysis System (SAS) (Cary, NC).

RESULTS

Intravenous Ketamine Anesthesia, Pharmacokinetics, and Physiologic Responses

Pharmacokinetics of ketamine. Steady-state plasma concentrations of ketamine were achieved following 6–12 h of anesthesia (Fig. 1A). The metabolite nor-ketamine also reached pseudosteady-state plasma levels by 12 h (Fig. 1B). PND 35 monkeys required a higher plasma concentration of ketamine to maintain the same plane of anesthesia as the PND 5 monkeys and pregnant adults. The metabolism of ketamine to nor-ketamine tended to occur more readily in infants than in adults.

Physiologic response to ketamine infusion. Maternal and infant physiological parameters including percent oxygen saturation, exhaled carbon dioxide, body temperature, heart rate, blood pressure, glucose, and hematocrit were all monitored and maintained within normal ranges. Small but statistically significant differences were observed between control and treated animals for some parameters. Heart rate was lower in all ketamine-treated monkeys than in the corresponding controls (Table 1). Respiratory rate was slower and expired

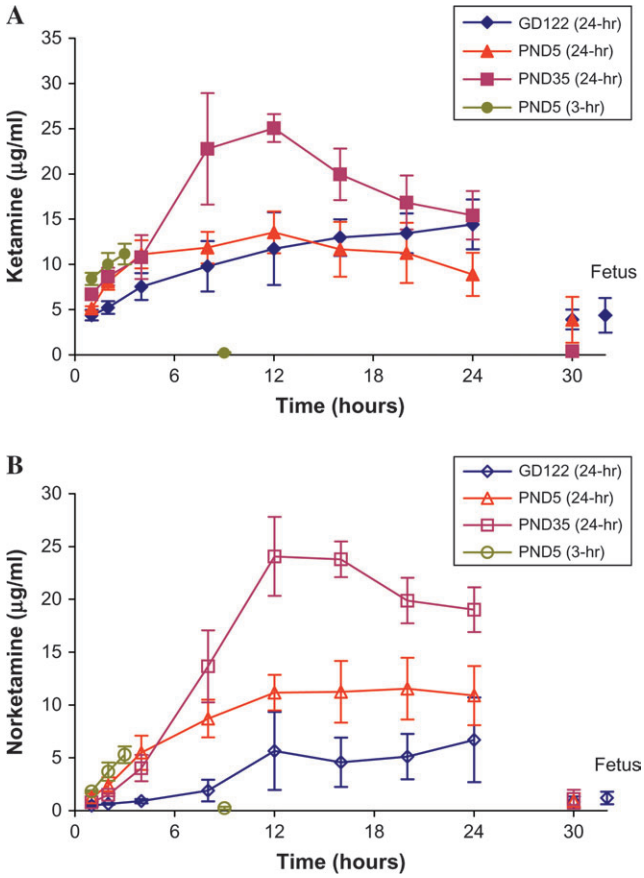

FIG. 1. Plasma concentrations of ketamine and nor-ketamine in pregnant (GD 122) or infant (PND 5 or PND 35) monkeys. Data points represent mean plasma concentrations (µg/ml) ± SEM for ketamine (A) and nor-ketamine (B) from monkeys infused with 20–50 mg/kg/h ketamine for 3 or 24 h, followed by a 6-h withdrawal period. Fetal plasma concentrations (GD 122) at the time of C-section of pregnant animals are indicated (fetus). $N = 3$ animals per time point.

CO_2 concentration was higher in treated than in control infants, and the changes were similar for PND 5 and PND 35 monkeys. Blood pressure was decreased in ketamine-treated pregnant females compared to controls, as well as in ketamine-treated PND 5 monkeys. The percent oxygen saturation averaged 94% or above for all study groups. Body temperature and blood glucose were not different between control and treated monkeys.

Anesthesia-Induced Neuronal Cell Death is Age (Developmental Stage) Dependent

Ketamine infusion for 24 h produces a large increase in the number of caspase 3–positive neurons in layers II and III of the frontal cortex in fetal (GD 122) (Fig. 2B) and PND 5 (Fig. 2D) infant monkey brains compared with control (Figs. 2A and 2C). Caspase 3–positive neurons in these layers still maintained typical pyramidal morphology and neuronal processes. Although a few caspase 3–positive neuronal cells were observed in some additional brain areas including the hippocampus, thalamus, striatum, and amygdala, no significant difference was detected between ketamine-treated and control monkeys in these areas (data not shown). Caspase 3–positive neurons were prominent in the cortex, especially in the frontal cortex in ketamine-treated monkeys (GD 122 and PND 5). Ketamine infusion had no effect in the cerebellum. In addition, no significant increase in cell death was observed in the brains of PND 35 monkeys treated with ketamine compared to control monkeys (Figs. 2E and 2F). As was the case for the caspase 3 expression pattern, increased numbers of Fluoro-Jade C–positive and Silver-impregnated degenerating neuronal cells were observed in the frontal cortex of GD 122 fetuses and PND 5 monkeys, but not in PND 35 monkeys (Fig. 3).

Anesthesia-Induced Neuronal Cell Death is Exposure-Time Dependent

At PND 5, 24-h ketamine infusions significantly increased the number of silver-impregnated neuronal cells (Fig. 4B) and the number of Fluoro-Jade C–positive degenerating neuronal cells (Fig. 4E) in layers II and III of the frontal cortex compared with controls (Figs. 4A and 4D). However, ketamine-induced

TABLE 1
Physiologic Parameters for Pregnant and Infant Monkeys Infused with Ketamine for 24 h or 3 h (PND 5 Infants Only)

	GD 122 (maternal)		PND 5 (infant)		PND 35 (infant)		PND 5 (infant)—3 h	
	Control	Ketamine	Control	Ketamine	Control	Ketamine	Control	Ketamine
Respiratory rate (bpm)	30 ± 5	36 ± 11	65 ± 13	43 ± 16*	72 ± 20	46 ± 25*	61 ± 13	52 ± 14
Expired CO_2	29 ± 6	31 ± 7	24 ± 2	33 ± 6*	22 ± 3	28 ± 5*	22 ± 2	30 ± 5*
Heart rate (bpm)	197 ± 32	130 ± 16*	219 ± 25	158 ± 26*	212 ± 34	171 ± 22*	237 ± 18	192 ± 17*
O_2 saturation (%)	94 ± 4	94 ± 4	96 ± 3	94 ± 3	97 ± 2	94 ± 3*	96 ± 2	94 ± 3
Temperature (°C)	37.3 ± 0.8	37.2 ± 0.9	36.9 ± 0.5	37.2 ± 0.8	36.8 ± 0.9	37.2 ± 0.7	36.6 ± 1.2	36.7 ± 0.8
MAP (mm Hg)	85 ± 13	68 ± 14*	63 ± 16	47 ± 10*	58 ± 16	53 ± 12	89 ± 26	47 ± 9*s
Glucose (mg/dl)	58 ± 15	48 ± 19	65 ± 12	56 ± 17	59 ± 27	58 ± 15	81 ± 50	66 ± 6
Hematocrit (%)	42 ± 3	42 ± 4	46 ± 5	43 ± 8	40 ± 6	36 ± 2	53 ± 2	41 ± 7*

Note. Values are means ± SD across all time points for $N = 3$ monkeys/group. MAP = mean arterial pressure. *Indicates significant difference ($p < 0.05$) between control and ketamine-treated monkeys for the same age and duration of exposure.

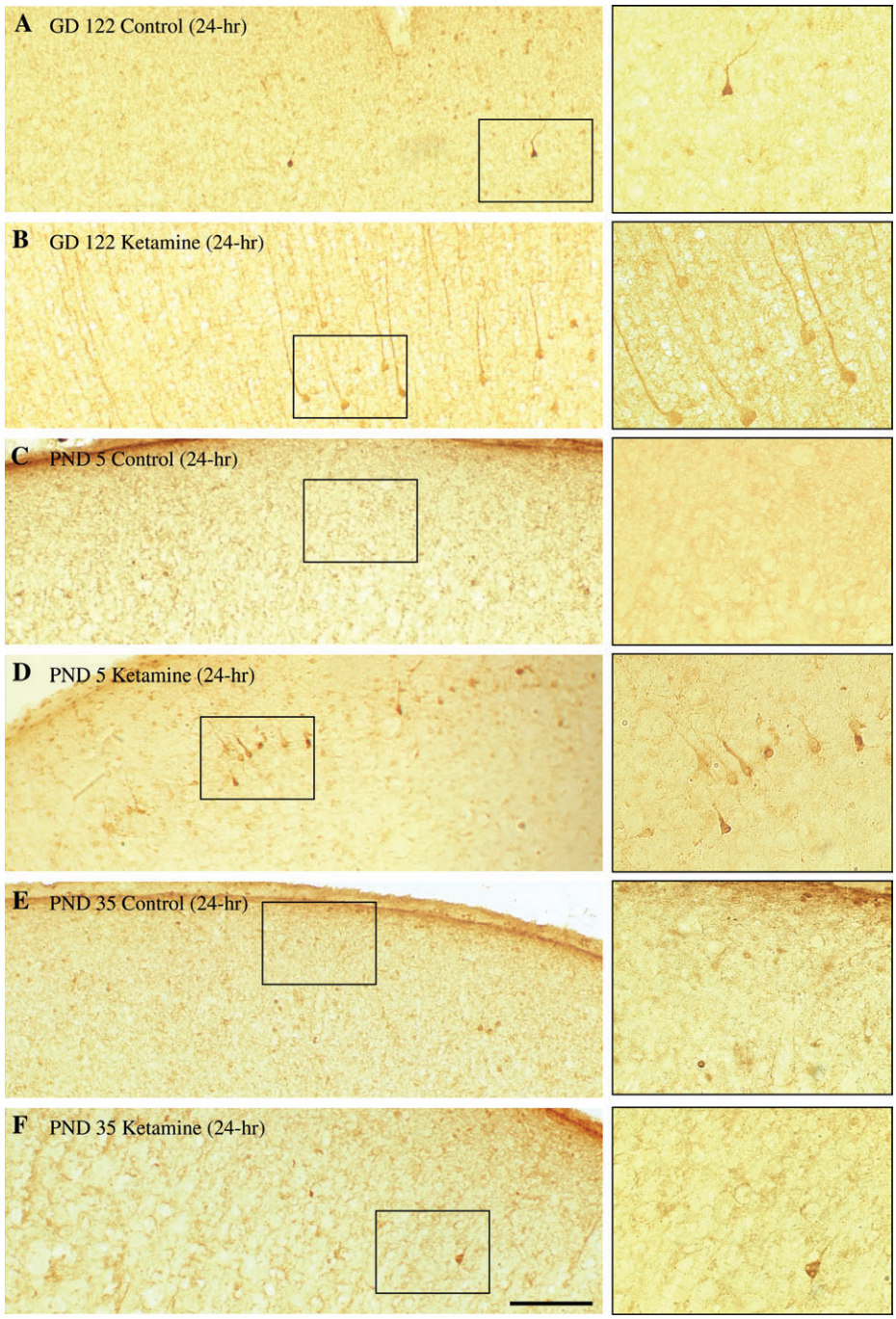

FIG. 2. Caspase 3 immunostaining in the frontal cortex of control and ketamine-treated monkeys. Intense caspase 3 immunostaining was observed in layers II and III neural cells in the ketamine-treated (24-h intravenous infusion) GD 122 (B) and PND 5 monkeys (D) compared to the controls (A and C). However, no significant increased number of caspase 3 positive neurons was observed in the ketamine-treated PND 35 monkeys (F) compared to controls (E). Scale bar = 100 μm

cell death was not detected in layers II and III in the frontal cortex of PND 5 monkeys infused with ketamine for only 3 h (Figs. 4C and 4F). Only a few Silver-, Fluoro-Jade C–, and caspase 3–positive neurons were observed in the hippocampus, thalamus, striatum, and amygdala and this was not different from control animals (data not shown). Statistical analyses of these data indicate that 24-h ketamine infusions, but not 3-h ketamine exposures, result in significant increases in the number of caspase 3–, Fluoro-Jade C– and silver stain–positive cells in the frontal cortex of PND 5 monkeys (Fig. 3).

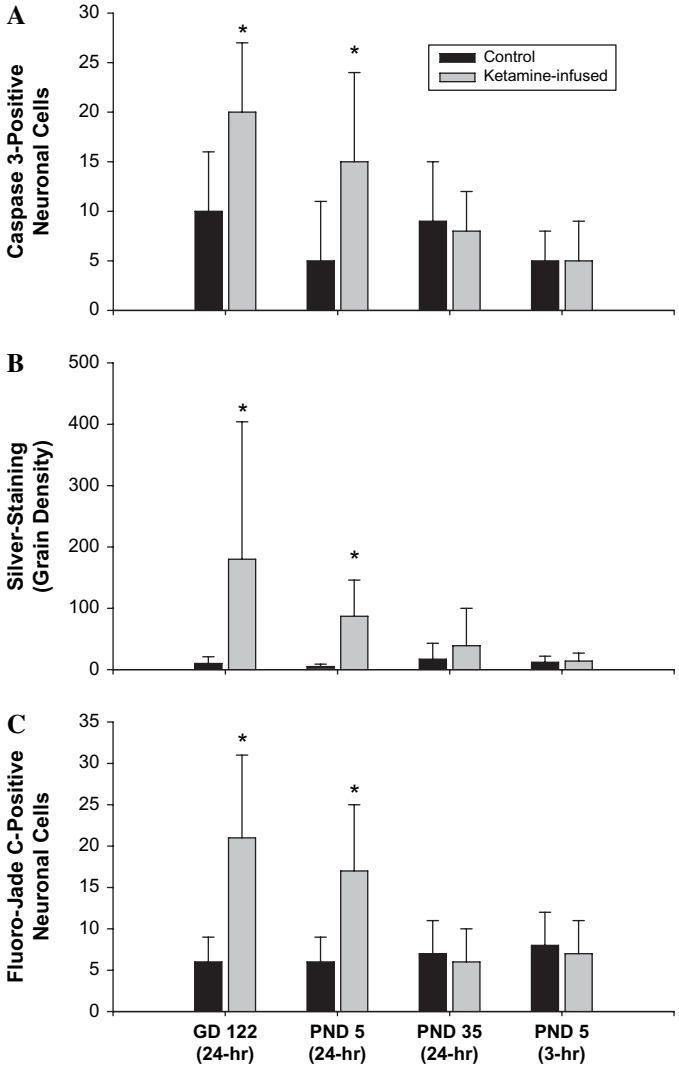

FIG. 3. Quantitative analyses of ketamine-induced neurodegeneration assessed using caspase 3 immunostaining (A), silver staining (B) and Fluoro-Jade C staining (C). For each condition, three animals were randomly assigned to treatment and control groups ($N = 3$/group). Data are presented as means ± SD. * A probability of $p < 0.05$ was considered significant (two-way ANOVA).

Anesthesia-Induced Neurodegeneration and Altered NMDA Receptor Expression

The 24-h ketamine infusions produced elevated neuronal cell death as indicated by the increased number of TUNEL-positive cells in GD 122 monkey fetuses and PND 5 infants. In controls (Fig. 5A), only a few TUNEL-positive cells were observed, however, numerous darkly stained TUNEL-positive cells exhibiting typical nuclear condensation and fragmentation indicative of enhanced apoptotic cell death were observed (Fig. 5B) in ketamine-infused PND 5 monkeys. The TUNEL assay relies on the detection of fragmented DNA strands. Although TUNEL assay is widely used to assess apoptosis *in situ*, it is not absolutely specific for apoptosis because fragmentation can occur via nonapoptotic mechanisms.

At the EM level, the direct evidence of increased neuronal cell death in PND 5 monkeys was confirmed, and no evidence of increased cell death was observed in PND 35 monkeys. Figure 6 shows representative nuclear condensation, fragmentation (apoptosis) (Fig. 6B-1), and necrotic characteristics (Fig. 6B-2), including neuronal mitochondrial swelling and neuronal cell body (with typical nucleolus in nucleus) swelling in the PND 5 monkeys compared to the controls that exhibit an intact cytoplasm and nuclear membrane (Fig. 6A).

In both controls and PND 5 ketamine-treated monkeys, NMDA receptor NR1 subunit mRNA is prominent (Fig. 7). The autoradiograph grain density (labeling) for NR1 subunit mRNA is upregulated in monkey infants treated with ketamine for 24 h (B) compared with controls (A). A comparison between the two indicates a significant increase for NR1 mRNA signals in ketamine-treated monkey infants. Quantitative analysis of the NR1 *in situ* hybridization signal indicates that no significant effect was observed between controls and monkey infants anesthetized for 3 h with ketamine (Fig. 7C).

DISCUSSION

Various anesthetic protocols have been used in pediatric medicine for many decades without clear systematic assessment concerning drug exposure and possible neurotoxicity. It is known that most of the currently used general anesthetic drugs have either NMDA receptor blocking or gamma-aminobutyric acid receptor enhancing properties. To minimize the risk to children resulting from the use of anesthetic agents, it is necessary to understand the effects of these drugs on the developing nervous system. While it is clear that ketamine causes neurodegeneration in the rodent model when given repeatedly during the brain growth-spurt period (Ikonomidou *et al.*, 1999; Wang *et al.*, 2005b), it is not yet known whether a similar phenomenon also occurs in primates. In order to better determine if ketamine-induced neurodegeneration in the developing rat has clinical relevance, ketamine was examined in a nonhuman primate model that more closely mimics the developing pediatric population (Haberny *et al.*, 2002; Wang *et al.*, 2006). The similarity of the physiology, pharmacology, metabolism, and reproductive systems of the nonhuman primate to that of the human, especially during pregnancy, allows the monkey to be an exceptionally good animal model for use in detecting potential neurodegenerative effects of ketamine.

In the present study, important maternal and infant physiological parameters including percent oxygen saturation, exhaled carbon dioxide, body temperature, heart rate, blood pressure, glucose, and hematocrit were all monitored and maintained within normal ranges. Monitoring and control of these parameters is an essential component of any animal model and is made possible by using a primate. The parameters are carefully controlled during pediatric anesthesia, but are very difficult to control and monitor in rodent models. Because

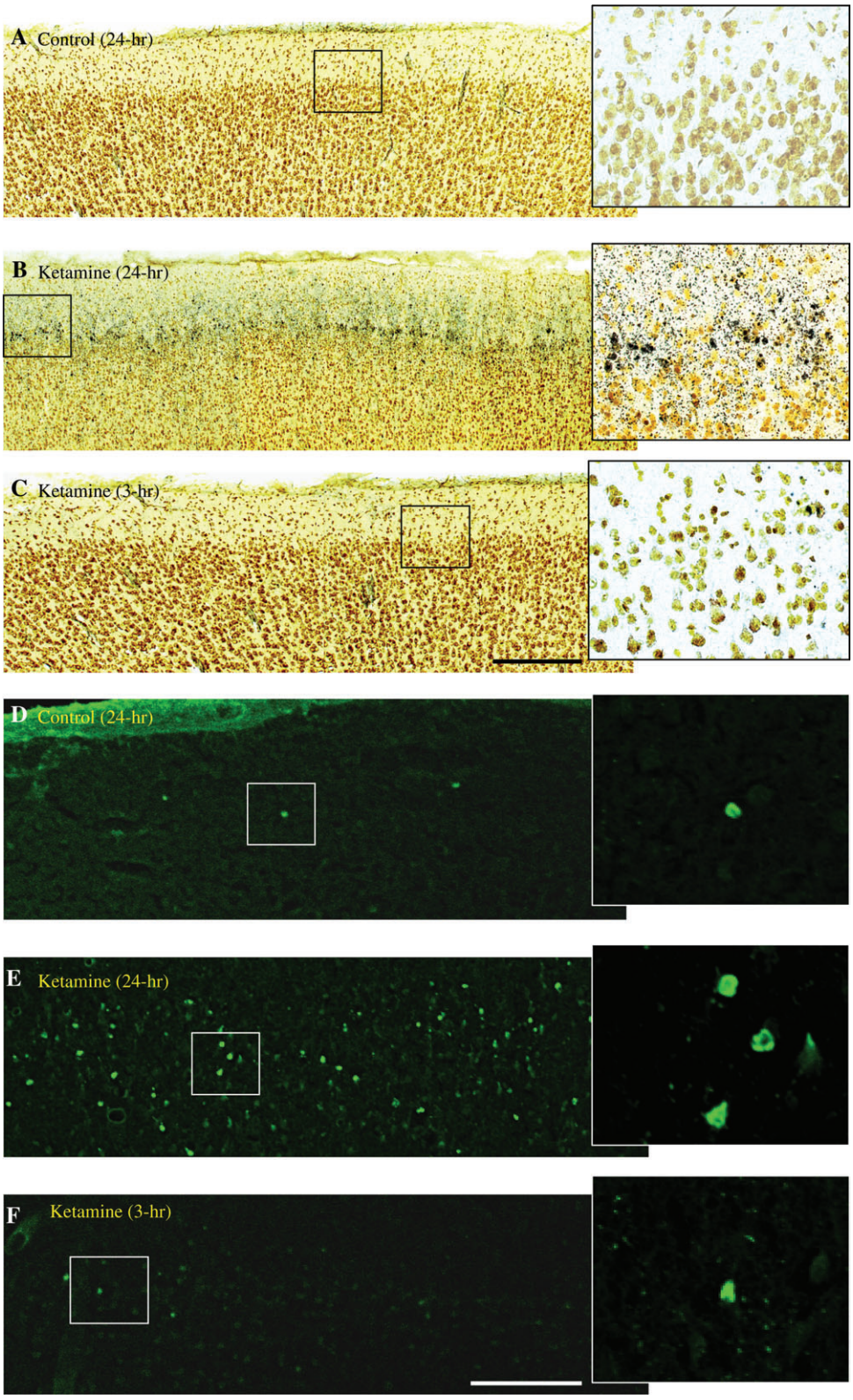

FIG. 4. Effects of ketamine infusion on Silver-impregnated neuronal cells and Fluoro-Jade C-positive neuronal cells. Increased numerical density of Silver-impregnated neuronal cells (B) and the number of Fluoro-Jade C–positive neuronal cells (E) were observed in layers II and III of the frontal cortex in 24-h ketamine-infused PND 5 monkeys compared with controls (A and D). However, no significant increased number of Silver-positive profiles and Fluoro-Jade C stained cells were observed in the 3-h ketamine-infused PND 5 monkeys (C and F).

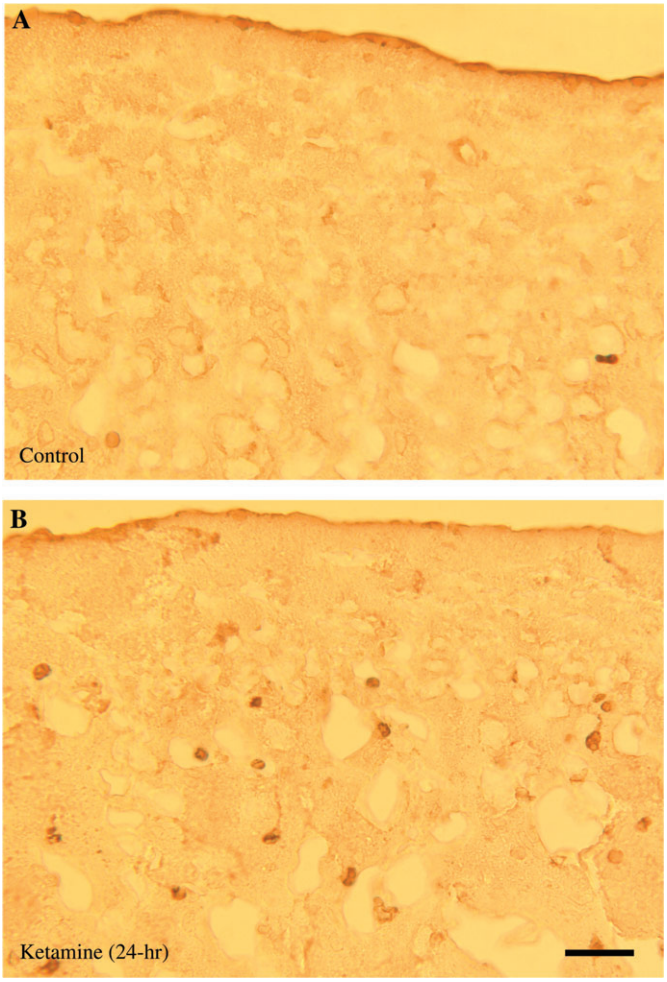

FIG. 5. Ketamine-induced neurodegeneration assessed by TUNEL labeling. Representative photographs indicate that TUNEL-positive cells are more numerous in layers II and III of the frontal cortex in 24-h ketamine-infused PND 5 monkeys (B). Only a few TUNEL-positive cells were observed in the PND 5 controls (A). Scale bar = 60 μm.

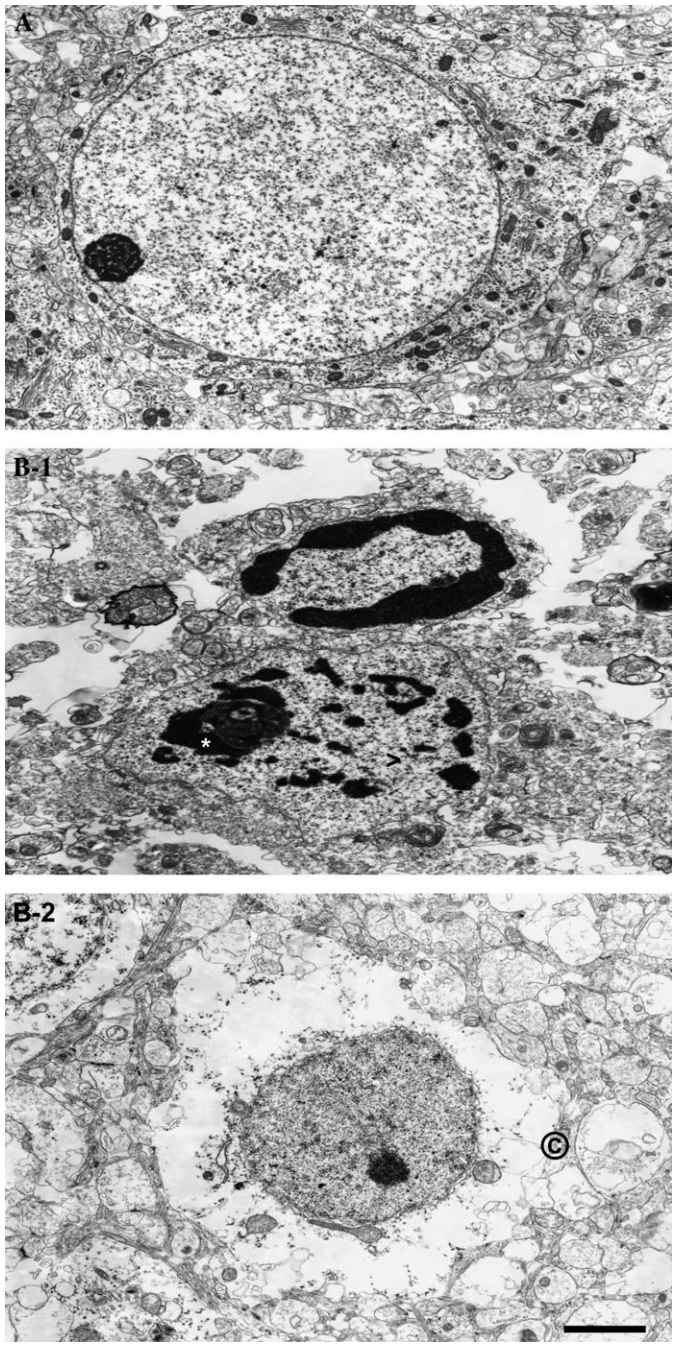

FIG. 6. Enhanced neuronal cell death in 24-h ketamine-infused monkeys. EM show a normal neuron with intact cytoplasm and nuclear membrane from a PND 5 control monkey (A). EMs also show nuclear condensation (*, in B-1), nuclear fragmentation (>, in B-1) (advanced states of apoptosis), typical mitochondrial swelling, and neuronal cell body swelling (©, in B-2) (necrosis) in layers II and III of the frontal cortex from a 24-h ketamine-infused PND 5 monkey. Scale bar = 0.64 μm.

prolonged hypoperfusion can lead to cerebral hypoperfusion and ischemic-related cell death, it is important that no evidence of abnormal blood pressure or oxygen saturation was observed. Ketamine is clinically used to provide anesthesia because it lacks the cardiorespiratory depression seen with most other general anesthetic agents (Zielmann *et al.*, 1997). Ketamine also possesses sympathomimetic properties which counteract the cardio-depressive properties of propofol (Badrinath *et al.*, 2000). In anesthetic practice, high plasma and brain concentrations of ketamine result in dissociative anesthesia, amnesia, a rise in arterial pressure, increased heart rate and cardiac output, and raised intracranial pressure with relative preservation of airway reflexes and respiration. Ketamine became established for use in hypovolemic patients and in difficult locations such as battlefields because of its relative safety. Thus, it is quite likely that the heart rate and blood pressure observed in the control animals were abnormally high due to the transient restraint stress associated with obtaining these measurements.

Placental transfer of ketamine occurs rapidly and maternal blood levels have been reported to be comparable to fetal blood

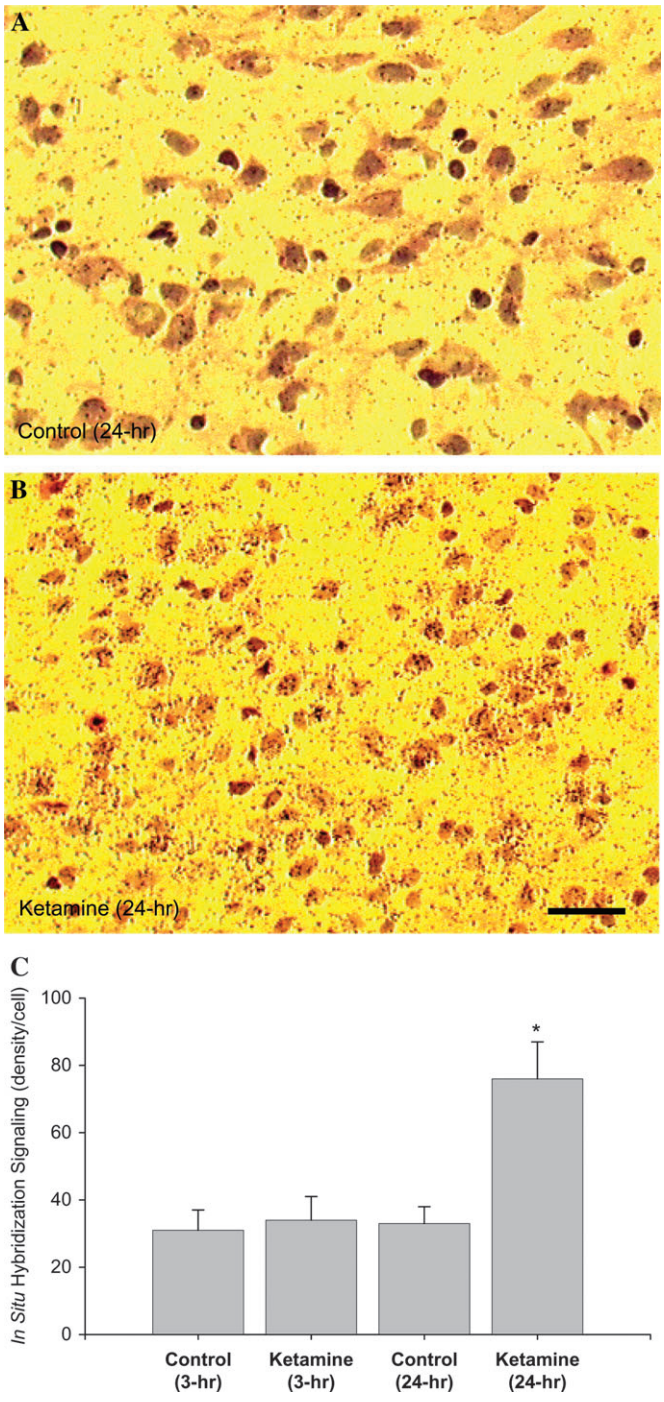

FIG. 7. NMDA receptor NR1 subunit mRNA abundance in the frontal cortex of PND 5 monkeys. The autoradiograph grain density (labeling) for NR1 subunit mRNA is upregulated in 24-h ketamine-infused monkeys (B) compared with controls (A). Quantitative analysis (relative labeling density) of the effects of ketamine infusion on the *in situ* hybridization signal of NMDAR1 subunit mRNA expression in layer II of the frontal cortex of PND 5 monkeys is also shown (C). A comparison between 24-h ketamine infusion and control indicates a significant increase ($*p < 0.05$) for NR1 mRNA *in situ* hybridization signals in ketamine-treated monkeys, however, no significant effect was observed between the 3-h ketamine-treated and control monkeys. Scale bar = 60 μm.

levels within 2 min of maternal administration (Ellingson *et al.*, 1977). Ketamine is distributed rapidly after intravenous administration (Grant *et al.*, 1981). Thereafter, plasma levels fall rapidly; however, the mean terminal half life is 186 ± 10 min, fitting a two compartment open model (Clements and Nimmo, 1981). In the present study, ketamine was given as an initial intramuscular injection (20 mg/kg) followed by a continuous intravenous infusion at a rate of 20–50 mg/kg/h. Peak plasma concentrations of ketamine were attained between 6 and 12 h after the beginning of infusion with peak concentrations of the metabolite nor-ketamine occurring slightly later. In the infants there appears to be greater metabolism of ketamine to nor-ketamine than in pregnant adults. The ketamine levels required to maintain anesthesia were 10–25 μg/ml, which is 5–10 times higher than those observed in humans (2–3 μg/ml). It is important to note that the plasma concentrations of ketamine were highest in the PND 35 monkeys even though no evidence of increased neuronal cell death was observed as compared to control animals of the same age. In the PND 5 monkeys, where neuronal cell loss was evident, the plasma levels averaged approximately 10 μg/ml, which is only three to five times the plasma levels observed in humans. It is noteworthy that the monkey requires higher plasma levels of ketamine to achieve the desired degree of anesthesia.

During the brain growth spurt, blockade of the NMDA receptor for a period of hours triggers widespread apoptotic neurodegeneration in the rodent brain (Jevtovic-Todorovic *et al.*, 2003). In the present study, potential neurodegenerative effects induced by ketamine were examined using caspase 3 immunostaining and degeneration-selective stains (Silver- and Fluoro-Jade C-stain). These data suggest that the earlier developmental stages in the monkey (GD 122 and PND 5) are more sensitive to ketamine-induced cell death than are later developmental stages, such as PND 35. It should be noted that the pattern or topography of ketamine-induced neurodegeneration in developing monkeys is very different from that reported in developing rodents. A previous study demonstrated significant increases in apoptosis in multiple brain regions, particularly in the thalamus, of the PND 7 rat pup after ketamine administration (Ikonomidou *et al.*, 1999). Also, the developmental lesions caused by ketamine are distinctly different from those that occur in adult rats, which are characterized by vacuole formation in the retrosplenial cortex (Olney, 1994). However, the consequences of altered apoptotic events during development may be far more serious than the lesions seen in adult animals because a larger proportion of brain neurons may be compromised. Thus, it is proposed that the topographic differences in ketamine-induced neurodegeneration may be related to (1) duration of anesthesia/exposure; (2) route of ketamine administration; (3) animal species; (4) ketamine plasma levels; and (5) the developmental stage at the time of exposure. Furthermore, there is considerable information on species differences concerning the ontogeny of glutamate receptors (Johnson, 1994). It is generally considered that NMDA receptor binding

sites are present in the human fetal brain by GD 115, increase until GD 140–150 and then decrease slightly by GD 168–182 (Haberny *et al.*, 2002). The localization of NMDA receptors in monkey cortices is similar to that seen in humans (Huntley *et al.*, 1997). In contrast, the distribution of NMDA receptors in rats is different from that in monkeys (Meoni *et al.*, 1998). An earlier study showed that there were differences between rats and monkeys with respect to the selective effects of NMDA receptor antagonists on specific learning processes (Cory-Slechta, 1994). Because the brain growth-spurt period in humans and nonhuman primates extends over a much longer period than in the rat, it is difficult to match between species the exact stage of development during which particular neurodevelopmental events occur. It should be noted that relative to birth, the rodent is immature as compared to the human or monkey so that early postnatal studies in the rat are comparable to late gestation or newborn status in the primate.

Although a complete definition of the window of vulnerability to the effects of ketamine in the primate is not possible from a single study, sensitivity is apparent from at least by 75% of gestation and lasts to early postnatal life up to sometime before PND 35. However, in the rat, the window of vulnerability begins one day after birth and ends approximately 14 days later (Ikonomidou *et al.*, 1999). This is a period in the rat before the complete development of motor and other relevant systems and during intense synaptic remodeling in multiple brain regions. This is also a period of rapid myelin formation during which most afferent pathways are already present in their target areas; however, their distribution and synaptic targets are still immature. During these sensitive stages, altered glutamatergic neurotransmission and receptor expression induced by NMDA antagonists (such as ketamine) could affect neuroplasticity and cause neuronal toxicity. Thus, abnormal neuronal development, abnormal synaptic plasticity, and neurodegeneration have been proposed as causal or contributing factors in anesthetic-induced neurotoxicity (Wang *et al.*, 2006). The period of vulnerability of the immature rat brain to ketamine-induced neurodegeneration coincides with the critical stages of monkey brain development. GD 122 fetuses and PND 5 infants that are at the peak of synaptogenesis, appear much more vulnerable than PND 35 monkeys that are undergoing much less synaptogenesis. Although the precise correlation between stages of brain development in humans and monkeys and/or species-specific vulnerabilities to anesthesia-induced neuronal damage cannot be specified, matching such events between human and nonhuman primates is less problematic than matching these phenomena between primates and rodents. For example, according to a recent review, the GD 123 monkey fetus is equivalent to the 199 GD human fetus as determined by cortical development and both are in the range of 75–80% of normal term (Clancy *et al.*, in press).

One of the main goals of this study was to determine whether there is an anesthetic duration below which no significant ketamine-induced neuronal cell death can be detected. In the present study, PND 5 monkeys were evaluated after 3 and 24 h of ketamine anesthesia. The 24-h duration was selected as a relatively long duration, while the 3-h duration more closely approximates typical general pediatric anesthesia. The results indicate that no significant neurotoxic effects were observed if the anesthesia duration was 3 h; however, 24-h anesthetic sessions produced a significant increase in the number of caspase 3–positive neurons, silver-stained and Fluoro-Jade C–positive cells in layers II and III of the cortex. These data are very consistent with those observed in our time-course studies using a primary cortical culture system established from developing rats and PND 3 monkeys (Wang *et al.*, 2005b, 2006). In these time-course studies, the cultures were exposed to ketamine for 2, 4, 6, 12, and 24 h and the data indicated that the addition of 10μM ketamine results in about a 30% loss in cell viability at 6 h, and an approximately 50–70% loss after 12–24 h of exposure. However, there were no significant differences between control and ketamine-exposed cultures at 2 h. After 4 h of exposure a slight but nonsignificant increase in cell death was observed. It was proposed that continuous activation of upregulated NMDA receptors (compensatory) over 6–24 h was critical for the production of ketamine-induced cell death in developing neurons in monkey frontal cortical cultures (Wang *et al.*, 2006).

The NMDA receptor NR1 subunit is widely distributed throughout the brain and is the fundamental subunit necessary for NMDA channel function. NMDA receptor density has been shown to increase in cultured cortical neurons after exposure to the NMDA receptor antagonists D-AP5, CGS-19755, and MK-801, but not after exposure to the alpha-amino-3-hydroxy-5-methyl-4-isoxazolepropionic acid/kainate receptor antagonist CNQX (Williams *et al.*, 1992). Overactivation of NMDA receptors is known to kill neurons via a necrotic mechanism characterized by excessive sodium and calcium entry, accompanied by chloride and water entry that leads to cell swelling and death (Rothman *et al.*, 1985). More recently, it has been shown that NMDA receptor activation can also lead to apoptotic cell death (Ankarkona *et al.*, 1995; Wang *et al.*, 2000, 2004). The characteristics of an excitotoxic insult that lead to necrosis or apoptosis are not clearly elucidated and may depend on the concentration of glutamate agonist, the duration of the treatment, the receptor subtype activated, and the cell type and its stage of development or maturity (Portera-Cailliau *et al.*, 1997). In previous studies we have observed that the administration of PCP, a noncompetitive NMDA antagonist, results in enhanced NMDA receptor expression and function *in vivo* and *in vitro* (Wang *et al.*, 1999, 2000). This also appears to be true for ketamine treatment *in vitro*. We found that ketamine administration to forebrain cultures also results in an upregulation of NMDA receptor NR1 subunit protein that is accompanied by enhanced apoptosis. Ketamine-induced apoptosis was confirmed by measuring the alterations in the number of TUNEL-positive cells, 3-(4,5-dimethylthiazole-2-yl)-2,5-diphenyltetrazolium bromide (MTT) metabolism, and DNA fragmentation. In addition, no significant effect was observed on lactate dehydrogenase

(LDH) release (indicating necrotic cell death) in ketamine-treated (10μM) rat cultures (Wang *et al.*, 2005b). In monkey frontal cortical cultures, however, ketamine produces a dose-related increase in neurotoxicity (Wang *et al.*, 2006). In contrast to the effects of ketamine in rat cultures, increased internucleosomal DNA fragments (mostly apoptotic) and significant increases in LDH release (mostly necrotic), coupled with decreased mitochondrial MTT metabolism (reduction of total cell viability), suggest that ketamine-induced cell death in monkey cultures is characterized by both apoptosis and necrosis. In the present study, to better understand the nature of ketamine-induced cell death in the developing primate brain, TUNEL data and EM observations in the prefrontal cortex were analyzed using tissue from PND 5 monkeys. The TUNEL-assay labels broken DNA strands, a process often associated with apoptosis. Numerous darkly stained TUNEL-positive cells were observed in 24-h, but, not in 3-h ketamine-infused monkeys (PND 5). EM observations showed typical nuclear condensation, fragmentation, and neuronal mitochondrial swelling, as well as neuronal cell body swelling in the 24-h ketamine-treated infants and fetuses, but not in monkey infants anesthetized for only 3 h. Although it was not the intent of this study to absolutely distinguish between apoptosis and necrosis, nor their apoptotic to necrotic ratios, these data support the hypothesis that ketamine-induced neuronal cell death in PND 5 monkey is both apoptotic and necrotic in nature.

The ability of ketamine to enhance neurodegeneration may be the result of a ketamine-induced compensatory upregulation of NMDA receptors. This upregulation makes neurons bearing these receptors more vulnerable, after ketamine withdrawal, to the excitotoxic effects of endogenous glutamate. In fact, this hypothesis was supported by the observation that, in cells (monkey *in vitro*) kept in defined serum-free media with no or very low concentrations of glutamate for 24 h after ketamine withdrawal, no significant effects of ketamine were noted. In addition, a 4- to 6-h minimum withdrawal (ketamine washout) period is necessary for ketamine-induced neurotoxicity *in vitro*, and the coadministration of antisense oligonucleotides that specifically target NMDA receptor NR1 subunit mRNA was able to block the neural damage induced by 10μM ketamine (Wang *et al.*, 2006).

Of particular interest are the possible mechanisms by which ketamine might upregulate NMDA receptors. In the present study, to determine whether altered regulation of NMDA receptor subunits promotes ketamine-induced cell death, *in situ* hybridization detecting the relative densities of NMDA receptor NR1 subunits following ketamine infusion was performed. An oligonucleotide probe complementary to the mRNA encoding the NMDA receptor NR1 subunit was selected (Monyer *et al.*, 1992; Moriyoshi *et al.*, 1991). Our present data indicate that in the monkey frontal cortex, NMDA receptor NR1 subunit mRNA is prominent, and labeling for NR1 subunit mRNA was upregulated in 24-h ketamine-treated monkeys (PND 5) compared with controls. Importantly, no significant effect on the expression of NR1 subunit mRNA was detected in PND 5 monkeys infused with ketamine for 3 h. These results are consistent with the literature demonstrating that treatment with NMDA antagonists produces upregulation of the NMDA receptor complex as measured by an increase in the B_{max} of NMDA receptor binding sites (McDonald *et al.*, 1990; Williams *et al.*, 1992). Chronic treatment with ethanol, another non-competitive NMDA antagonist (Lovinger *et al.*, 1989), has also been shown to upregulate NMDA receptor number and function both *in vitro* and *in vivo* (Grant *et al.*, 1990; Trevisan *et al.*, 1994). Together these results indicate that NMDA antagonists are capable of increasing the amount of receptor message as well as elevating neuronal cell death. It is possible that the increased NR1 expression seen here was due to an increase in the rate of transcription or a decrease in the rate of degradation. Since the exact relationship between receptor subunit mRNA and protein expressed in the cell membrane is unknown, alterations in the mRNA level cannot be interpreted as alterations in NMDA receptor subunit expression. Although, a change in mRNA synthesis could result in increased receptor expression, it has been reported that chronic ingestion of ethanol over a 12-week period results in an increase in NR1 immunoreactivity in hippocampus, but not in the cortex, nucleus accumbens, or striatum (Trevisan *et al.*, 1994). Thus, the pattern of changes in the regulation of NMDA receptor expression may be quite different, depending on the antagonist, and the dose, duration, and frequency of its administration and species. In addition, it is possible that an increased expression of NR1 was accompanied by an altered expression of other subunits. Furthermore, the subunit composition and functional properties of NMDA receptors are developmentally regulated (Flint *et al.*, 1997; Zhong *et al.*, 1996). NMDA receptors in immature rat brain mediate longer-duration excitatory postsynaptic potentials and are less sensitive to Mg^{2+} block and more sensitive to the coagonist glycine than mature NMDA receptors (Burgard and Hablitz, 1993; McDonald *et al.*, 1989). These specific characteristics may underlie the enhanced capacity of the developing brain for learning and plasticity (Flint *et al.*, 1997); however, they are also likely to increase the vulnerability of the postnatal brain to excitotoxic injury. It has been reported that exposure of developing rats to MK-801, a noncompetitive NMDA channel blocker, increases expression of NMDA receptor subunit mRNA (especially for NR2A) and mGluR5 mRNA, and this increase in gene expression for NMDA receptor subunits may contribute to the increased binding to NMDA receptors and the increased vulnerability to excitotoxic injury observed 24 h after MK-801 exposure (Wilson *et al.*, 1998).

Given the key role of the essential subunit, NR1, it is not surprising that in frontal cortex the upregulation of NR1 expression along with alterations in other NMDA receptor subunits (such as the NR2 family) play an important role in determining the pharmacological properties of the receptor. It has also been postulated that the excitotoxic effects of glutamate are largely mediated by increased Ca^{2+} influx through activated NMDA

receptors (Choi, 1987). Associated with this increased Ca^{2+} influx is an increase in the generation of reactive oxygen species (ROS) that appears to originate in mitochondria (Malis and Bonventre, 1985). Ca^{2+} loading by the mitochondria beyond their buffering capacity reduces their membrane potentials and disrupts electron transport which results in the increased production of the reactive free radical superoxide anion $O_2^{\cdot-}$ (Luetjens *et al.*, 2000). The present data suggest that continuously blocking the NMDA receptor in the developing brain with NMDA antagonists such as ketamine causes a compensatory upregulation of NMDA receptors. Therefore, the neurons bearing these receptors become more vulnerable, after ketamine withdrawal, to the excitotoxic effects of glutamate, because this upregulation of NMDA receptors allows for the accumulation of toxic levels of intracellular Ca^{2+} under normal physiological conditions.

Taken together, the data suggest that long-term (24 h) ketamine exposure–induced neuronal cell death in the perinatal monkey brain is most likely both apoptotic and necrotic in nature. Ketamine-induced cell death may involve the upregulation of the NMDA receptor NR1 subunit mRNA during development. The earlier developmental stages (GD 122 and PND 5) are more sensitive to anesthetic-induced neurodegeneration than are later developmental stages, such as PND 35. Importantly, the present study has demonstrated that shorter duration anesthesia (ketamine infusion for 3 h) does not produce neuronal cell death in the PND 5 monkey.

ACKNOWLEDGMENTS

This work was supported by the NCTR/U.S. Food and Drug Administration (FDA), Center for Drug Evaluation and Research/FDA, and the National Institute of Child Health and Human Development. The authors thank Dr. James Chen for his assistance with the statistical analyses.

REFERENCES

Ankarkona, M. M., Dybukt, J. M., Bonfoko, E., Zhivotovsky, B., Orrenius, S., Lipton, S. A., and Nicotera, P. (1995). Glutamate-induced neuronal death: A succession of necrosis or apoptosis depending on mitochondrial function. *Neuron* **15,** 961–973.

Badrinath, S., Avramov, M. N., Shadrick, M., Witt, T. R., and Ivankovich, A. D. (2000). The use of a ketamine-propofol combination during monitored anesthesia care. *Anesth. Analg.* **90,** 858–862.

Bartanusz, V., Jezova, D., Bertini, L. T., Tilders, F. J. H., Aubry, J. M., and Kiss, J. Z. (1993). Stress-induced increase in vasopressin and corticotrophin-releasing factor expression in hypophysiotrophic paraventricular neurons. *Endocrinology* **132,** 895–902.

Beal, M. F. (1992). Mechanisms of excitotoxicity in neurologic diseases. *FASEB J.* **6,** 3338–3344.

Burgard, E. C., and Hablitz, J. J. (1993). Developmental changes in NMDA and non-NMDA receptor-mediated synaptic potentials in rat neocortex. *J. Neurophysiol.* **69,** 230–240.

Choi, D. W. (1987). Ionic dependence of glutamate neurotoxicity. *J. Neurosci.* **7,** 369–379.

Clancy, B., Finlay, B. L., Darlington R. B., and Anand K. J. S. Extrapolating brain development from experimental species to humans. *NeuroToxicology* (in press).

Clements, J. A., and Nimmo, W. S. (1981). Pharmacokinetics and analgesic effect of ketamine in man. *Br. J. Anaesth.* **53,** 27–30.

Collingridge, G. L., Kehl, S. J., and McLennan, H. (1983). Excitatory amino acids in synaptic transmission in the Schaffer collateral-commissural pathway of the rat hippocampus. *J. Physiol.* **334,** 33–46.

Cory-Slechta, D. A. (1994). The impact of NMDA receptor antagonists on learning and memory functions. *Psychopharmacol. Bull.* **30,** 601–612.

D'Souza, S. W., McConnell, S. E., Slater, P., and Barson, A. J. (1993). Glycine site of the excitatory amino acid N-methyl-D-aspartate receptor in neonate and adult brain. *Arch. Dis. Child.* **69,** 212–215.

Ellingson, A., Haram, K., Sagen, N., and Solheim, E. (1977). Transplacental passage of ketamine after intravenous administration. *Acta Anaesthesiol. Scand.* **21,** 41–44.

Flint, A. C., Maisch, U. S., Weishaupt, J. H., Kriegestein, A. R., and Monyer, H. (1997). NR2A subunit expression shortens NMDA receptor synaptic currents in developing neocortex. *J. Neurosci.* **17,** 2469–2476.

Grant, I. S., Nimmo, W. S., and Clements, J. A. (1981). Lack of effect of ketamine analgesia on gastric emptying in man. *Br. J. Anaesth.* **53,** 1321–1323.

Grant, K. A., Valverius, P., Hudspith, M., and Tabakoff, B. (1990). Ethanol withdrawal seizures and the NMDA complex. *Eur. J. Pharmacol.* **176,** 289–296.

Haberny, K. A., Paule, M. G., Scallet, A. C., Sistare, F. D., Lester, D. S., Hanig, J. P., and Slikker, W. Jr. (2002). Ontogeny of the N-methyl-D-aspartate (NMDA) receptor system and susceptibility of neurotoxicity. *Toxicol. Sci.* **68,** 9–17.

Hanania, T., Hillman, G. R., and Johnson, K. M. (1999). Augmentation of locomotor activity by chronic phencyclidine is associated with an increase in striatal NMDA receptor function and an upregulation of the NR1 receptor subunit. *Synapse* **31,** 229–239.

Huntley, G. W., Vickers, J. C., and Morrison, J. H. (1997). Quantitative localization of NMDAR1 receptor subunit immunoreactivity in inferotemporal and prefrontal association cortices of monkey and human. *Brain Res.* **749,** 245–262.

Ikonomidou, C., Bosch, F., Miksa, M., Bittigau, P., Vockler, J., Dikranian, K., Tenkova, T. I., Stefovska, V., Turski, L., and Olney, J. W. (1999). Blockade of NMDA receptors and apoptotic neurodegeneration in the developing brain. *Science* **283,** 70–74.

Jevtovic-Todorovic, V., Hartman, R. E., Izumi, Y., Benshoff, N. D., Dikranian, K., Zorumski, C. F., Olney, J. W., and Wozniak, D. F. (2003). Early exposure to common anesthetic agents causes widespread neurodegeneration in the developing rat rain and persistent learning deficits. *J. Neurosci.* **23,** 876–882.

Johnson, K. M., Phillips, M., Wang, C., and Kevetter, G. A. (1998). Chronic phencyclidine induces behavioral sensitization and apoptotic cell death in the olfactory and piriform cortex. *J. Neurosci. Res.* **52,** 709–722.

Johnson, M. V. (1994). Developmental aspects of NMDA receptor agonists and antagonists in the central nervous system. *Psychopharmacol. Bull.* **30,** 567–575.

Kohrs, R., and Durieux, M. E. (1998). Ketamine: Teaching an old drug new tricks. *Anesth. Analg.* **87,** 1186–1193.

Kutsuwada, T., Kashiwabuchi, N., Mori, H., Sakimura, D., Kushiya, E., Araki, K., Meguro, H., Masaki, H., Kumanishi, G., Arakawa, M., and Mishina, M. (1992). Molecular diversity of the NMDA receptor channel. *Nature* **358,** 36–41.

Laurie, D. J., and Seeburg, P. H. (1994). Regional and developmental heterogeneity in splicing of the rat brain NMDAR1 mRNA. *J. Neurosci.* **14,** 3180–3194.

Lovinger, D. M., White, G., and Weight, F. F. (1989). Ethanol inhibits NMDA-activated ion current in hippocampal neurons. *Science* **243,** 1721–1724.

Luetjens, C. M., Bui, N. T., Sengpiel, B., Munstermann, G., Poppe, M., Krohn, A. J., Bauerbach, E., Krieglstein, J., and Prehn, J. H. (2000). Delayed mitochondrial dysfunction in excitotoxic neuron death: Cytochrome c release and secondary increase in superoxide production. *J. Neurosci.* **20,** 5715–5723.

Malis, C. D., and Bonventre, J. V. (1985). Mechanism for calcium potentiation of oxygen free radical injury to renal mitochondria. *J. Biol. Chem.* **261,** 14201–14208.

McDonald, J. W., Roeser, N. F., Silverstein, F. S., and Johnston, M. V. (1989). Quantitative assessment of neuroprotection against NMDA-induced brain injury. *Exp. Neurol.* **106,** 289–296.

McDonald, J. W., Silverstein, F. S., and Johnston, M. V. (1990). MK-801 pretreatment enhances N-methyl-D-aspartate brain injury and increases brain N-methyl-D-aspartate recognition site binding in rats. *Neuroscience* **38,** 103–113.

Meldrum, B., and Garthwaite, J. (1990). Excitatory amino acid neurotoxicity and neurodegenerative disease. *Trends Pharmacol. Sci.* **11,** 379–387.

Mellon, R. D., Simone A. F., and Rappaport, B. A. (2007). Use of anesthetic agents in neonates and young children. *Anesth. Analg.* **104**(3), 509–520.

Meoni, P., Bunemann, B. H., Trist, D. G., and Bowery, N. G. (1998). N-terminal splices variants of the NMDAR1 glutamate receptor subunit: Differential expression in human and monkey brain. *Neurosci. Lett.* **249,** 45–48.

Monyer, H., Sprengel, R., Schoepfer, R., Herb, A., Higuchi, M., Lomeli, H., Burnashev, N., Sakmann, B., and Seeburg, P. H. (1992). Heteromeric NMDA receptors: Molecular and functional distinction of subtypes. *Science* **256,** 1217–1221.

Moriyoshi, K., Masu, M., Ishii, T., Shigemoto, R., Mizuno, N., and Nakanishi, S. (1991). Molecular cloning and characterization of the rat NMDA receptor. *Nature* **354,** 31–37.

Muller, D., Wang, C., Skibo, G., Toni, N., Cremer, H., Calaora, V., Rougon, G., and Kiss, J. Z. (1996). PSA-NCAM is required for activity-induced synaptic plasticity. *Neuron* **17,** 413–422.

Nishi, M., Hinds, H., Lu, H. P., Kawata, M., and Hayashi, Y. (2001). Motoneuron-specific expression of NR3B, a novel NMDA-type glutamate receptor subunit that works in a dominant-negative manner. *J. Neurosci.* **21,** RC185.

Olney, J. W. (1994). Neurotoxicity of NMDA receptor antagonists: An overview. *Psychopharmacol. Bull.* **30,** 533–540.

Paxinos, G., Huang, X. F., and Toga, A. W. (2000). *The Rhesus Monkey Brain in Stereotaxic Coordinates.* Academic Press, A Harcourt Science and Technology Company, San Diego, CA.

Portera-Cailliau, C., Price, D. L., and Martin, L. J. (1997). Non-NMDA and NMDA receptor-mediated excitotoxic neuronal deaths in adult brain are morphologically distinct: Further evidence for an apoptosis-necrosis continuum. *J. Comp. Neurol.* **378,** 88–104.

Rabacchi, S. A., Bonfanti, L., Liu, X. H., and Maffei, L. (1994). Apoptotic cell death induced by optic nerve lesion in the neonatal rat. *J. Neurosci.* **14,** 5292–5301.

Rothman, D. L., Behar, K. L., Hetherington, H. P., den Hollander, J. A., Bendall, M. R., Petroff, O. A., and Shulman, R. G. (1985). ^{1}H-observe/^{13}C-decouple spectroscopic measurements of lactate and glutamate in the rat brain *in vivo. Proc. Natl. Acad. Sci. U.S.A.* **82,** 1633–1637.

Scallet, A., Schmued, L. C., Slikker, W., Grunberg, N., Faustino, P. J., Davis, H., Lester, D., Pine, P. S., Sistare, F., and Hanig, J. P. (2004). Developmental neurotoxicity of ketamine: Morphometric confirmation, exposure parameters, and multiple fluorescent labeling of apoptotic neurons. *Toxicol. Sci.* **81,** 364–370.

Schmued, L. C., Stowers, C. C., Scallet, A. C., and Xu, L. (2005). Fluoro-Jade C results in ultra high resolution and contrast labeling of degenerating neurons. *Brain Res.* **1035,** 24–31.

Trevisan, L., Fitzgerald, L. W., Brose, N., Gasic, G. P., Heinemann, S. F., Duman, R. S., and Nestler, E. J. (1994). Chronic ingestion of ethanol upregulates NMDAR1 receptor subunit immunoreactivity in rat hippocampus. *J. Neurochem.* **62,** 1635–1638.

Wang, C., Anastasio, N., Popov, V., LeDay, A., and Johnson, K. M. (2004). Blockade of N-methyl-D-aspartate receptors by phencyclidine causes the loss of corticostriatal neurons. *Neuroscience* **125,** 473–483.

Wang, C., Fridley, J., and Johnson, K. M. (2005a). The role of NMDA receptor upregulation in phencyclidine-induced cortical apoptosis in organotypic culture. *Biochem. Pharmacol.* **69,** 1373–1383.

Wang, C., Kaufmann, J. A., Sanchez-Ross, M. G., and Johnson, K. M. (2000). Mechanisms of N-methyl-D-aspartate-induced apoptosis in phencyclidine-treated cultured forebrain neurons. *J. Pharmacol. Exp. Ther.* **294,** 287–295.

Wang, C., McInnis, J., West, J. B., Bao, J., Anastasio, N., Guidry, J. A., Ye, Y., Salvemini, D., and Johnson, K. M. (2003). Blockade of phencyclidine-induced cortical apoptosis and deficits in prepulse inhibition by M40403, a superoxide dismutase mimetic. *J. Pharmacol. Exp. Ther.* **304,** 266–271.

Wang, C., Showalter, V. M., Jillman, G. R., and Johnson, K. M. (1999). Chronic phencyclidine increases NMDA receptor NR1 subunit mRNA in rat forebrain. *J. Neurosci. Res.* **55,** 7762–7769.

Wang, C., Sadovova, N., Fu, X., Scallet, A., Hanig, J., and Slikker W. (2005b). The role of NMDA receptors in ketamine-induced apoptosis in rat forebrain culture. *Neuroscience* **132,** 967–977.

Wang, C., Sadovova, N., Hotchkiss, C., Fu, X., Scallet, A. C., Patterson, T. A., Hanig, J., Paule, M. G., and Slikker, W., Jr. (2006). Blockade of N-methyl-D-aspartate receptors by ketamine produces loss of postnatal day 3 monkey frontal cortical neurons in culture. *Toxicol. Sci.* **91,** 192–201.

Williams, K., Dichter, M. A., and Molinoff, P. B. (1992). Up-regulation of N-methyl-D-aspartate receptors on cultured cortical neurons after exposure to antagonists. *Mol. Pharmacol.* **42,** 147–151.

Wilson, M. A., Kinsman, S. L., and Johnston, M. V. (1998). Expression of NMDA receptor subunit mRNA after MK-801 treatment in neonatal rats. *Dev. Brain Res.* **109,** 211–220.

Wong, H. K., Liu, X. B., Matos, M. F., Chan, S. F., Perex-Otano, I., Boysen, M., Cui, J., Nakanishi, N., Trimmer, J. S., Jones, E. G., Lipton, S. A., and Sucher, N. J. (2002). Temporal and regional expression of NMDA receptor subunit NR3A in the mammalian brain. *J. Comp. Neurol.* **450,** 303–317.

Ye, X., Carp, R. I., Schmued, L. C., and Scallet, A. C. (2001). Fluoro-Jade and silver methods: Application to the neuropathology of scrapie, a transmissible spongiform encephalopathy. *Brain Res. Brain Res. Protoc.* **8,** 104–112.

Zhong, J., Gribkoff, V. K., and Molinoff, P. B. (1996). Use of subunit-specific antisense oligodeoxynucleotides to define developmental changes in the properties of N-methyl-D-aspartate receptors. *Mol. Pharmacol.* **50,** 631–638.

Zielmann, S., Kazmaier, S., Schnull, S., and Weyland, A. (1997). S-(+)-ketamine and circulation. *Anaesthesist* **46**(Suppl. 1), 43–46.